© 2015. Published by The Company of Biologists Ltd | Development (2015) 142, 953-961 doi:10.1242/dev.117986

RESEARCH ARTICLE

Geometric control of ciliated band regulatory states in the sea urchin embryo

Julius C. Barsi[1,*], Enhu Li[1,2,*] and Eric H. Davidson[1,‡]

ABSTRACT

The trapezoidal ciliated band (CB) of the postgastrular sea urchin embryo surrounds the oral ectoderm, separating it from adjacent embryonic territories. Once differentiated, the CB is composed of densely arranged cells bearing long cilia that endow the larva with locomotion and feeding capability. The spatial pattern from which the CB will arise is first evidenced during pregastrular stages by expression of the pioneer gene *onecut*. Immediately after gastrulation, the CB consists of four separate regulatory state domains, each of which expresses a unique set of transcription factors: (1) the oral apical CB, located within the apical neurogenic field; (2) the animal lateral CB, which bilaterally separates the oral from aboral ectoderm; (3) the vegetal lateral CB, which bilaterally serves as signaling centers; and (4) the vegetal oral CB, which delineates the boundary with the underlying endoderm. Remarkably, almost all of the regulatory genes specifically expressed within these domains are downregulated by interference with SoxB1 expression, implying their common activation by this factor. Here, we show how the boundaries of the CB subdomains are established, and thus ascertain the design principle by which the geometry of this unique and complex regulatory state pattern is genomically controlled. Each of these boundaries, on either side of the CB, is defined by spatially confined transcriptional repressors, the products of regulatory genes operating across the border of each subdomain. In total this requires deployment of about ten different repressors, which we identify in this work, thus exemplifying the complexity of information required for spatial regulatory organization during embryogenesis.

KEY WORDS: Sea urchin embryogenesis, Spatial gene expression, Transcriptional repression, Neurogenic ectoderm

INTRODUCTION

The spatial specification of the ciliated band (CB) from the sea urchin embryo presents a uniquely challenging regulatory problem. During late embryogenesis this band consists of ciliated cells that facilitate feeding and locomotion in the larva (Fig. 1A). Not only do these cells overlie axonal tracts descending from apical neurons, but also the CB per se constitutes a neurogenic territory (Yaguchi et al., 2010; Angerer et al., 2011). Long before differentiation of these cell types occurs, prior to gastrulation the future position of the CB is foreshadowed by expression of the gene *onecut*, erroneously referred to earlier as *hnf6* (Howard-Ashby et al., 2006), in a trapezoidal CB pattern four to five cells wide (Fig. 1B,C) (Otim et al., 2004; Poustka et al., 2004, 2007). When viewed from the oral side (as in Fig. 1C) the band of *onecut* expression can be seen to border the oral ectoderm on either side, to abut the endoderm vegetally, and in its animalmost portion to include the oral part of the apical neurogenic field.

Previous studies concerning the spatial specification of this band of gene expression did not address its heterogeneous nature and have primarily focused on the influence of signals in positioning the band, in particular TGFβ family ligands and their antagonists, including Nodal and Bmp2/4 (Duboc et al., 2004, 2008; Lapraz et al., 2009; Saudemont et al., 2010; Yaguchi et al., 2010; Angerer et al., 2011). However, it is not possible to elucidate from signal responses alone the transcriptional inputs into *onecut*, nor into the other regulatory genes that, as we show below, are also expressed in parallel within the CB. It is their transcriptional inputs, encoded directly in the genomic target site sequences of these genes, that govern their spatial expression. The genomically encoded CB gene expression pattern can only be understood by identifying these inputs. Spatial control of the CB gene expression pattern is unlikely to operate in a simple manner. As it traverses the embryo, this band forms the boundary between distinct, Boolean embryonic domains, each expressing a different regulatory state and each destined toward a different developmental fate. The various (indirect) effects of different signals and their antagonists on the disposition and breadth of the CB suggest that several different repressors might be responsible for confining its boundaries. The signals received in given territories can be expected to activate positively or negatively acting regulatory genes, but the diverse territories bordering the CB express unique regulatory states that result from different gene regulatory networks (GRNs) (Su et al., 2009; Li et al., 2012, 2014; Ben-Tabou de-Leon et al., 2013; Materna et al., 2013); consequently, regional regulatory inputs into the CB are also likely to differ. The regulatory system affecting overall CB disposition in the embryo could thus be predicted *a priori* to be complex. But just how complex, as revealed in the following studies, we were nonetheless surprised to discover.

Here we show that as gastrulation commences the CB regulatory state includes more genes than *onecut* alone and, more significantly, that gene expression in the CB is mosaic. Each of the four regions of the CB expresses a unique regulatory state by 24 hours post fertilization (hpf), yet all express *onecut* and *z166* (supplementary material Fig. S1F,J). Therefore, multiple boundaries of CB gene expression have to be accounted for, in that each of the four regulatory states of the band confronts a unique pair of distinct GRNs operating across its borders.

RESULTS

Regulatory states of the CB and of the neighboring territories

It is interesting to consider *a priori* the regulatory constraints on CB positioning. Each of the territories it borders has a distinct, known regulatory state. Indeed, as Fig. 2 shows, the expression domains of a number of regulatory genes specific to the territories that border the CB directly abut the transcriptional territories where

[1]Division of Biology and Biological Engineering, Caltech, Pasadena, CA 91125, USA. [2]Warp Drive Bio, LLC, 400 Technology Square, Cambridge, MA 02139, USA.
*These authors contributed equally to this work

[‡]Author for correspondence (davidson@caltech.edu)

Received 18 September 2014; Accepted 28 December 2014

Development (2015) 142, 953-961 doi:10.1242/dev.117986

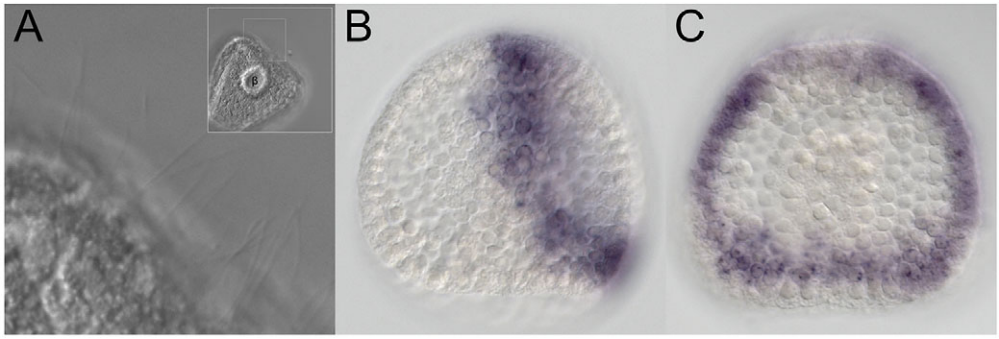

Fig. 1. The larval CB and its embryonic precursor. (A) Sea urchin larva at 72 hpf as viewed by DIC microscopy. High magnification along the vegetal oral margin of the larva partially reveals the CB. Low magnification (inset) shows the visible portion of the CB (white box) relative to the location the blastopore (β). (B,C) Pattern of gene expression revealed by RNA *in situ* hybridization. The zygotic expression pattern of the regulatory gene *onecut*, shown here at 25 hpf, is the first to delineate the CB (as early as 24 hpf). (B) Lateral view. (C) Oral view. The internal domain surrounded by the CB consists of oral ectoderm, although this itself is divided along the animal (top)/vegetal (bottom) axis into several subdomains (Li et al., 2014).

onecut is expressed. Fig. 2A,B provide a map of CB subdomains that we utilize in the following, while Fig. 2D-I show double RNA *in situ* hybridizations that illustrate this point: Fig. 2D,F demonstrate that the aboral ectoderm regulator *irxa* directly abuts the *onecut* stripe in subdomains 1 and 2; Fig. 2G,I demonstrate that the oral ectoderm regulator *gsc* directly abuts the *onecut* pattern in all subdomains; and Fig. 2E,H illustrate by reference to the Veg2 endoderm regulator *foxa* that subdomain 4 is coincident with Veg1 ectoderm but excluded from Veg1 endoderm (see legend). With respect to the domain of *onecut* expression per se, which is the subject of Fig. 2, there are two possible regulatory scenarios. Upstream regulatory genes expressed in the same pattern as *onecut*, or in respective portions of its overall pattern, could drive its expression; or, it could obey a broadly distributed activator and have its boundaries set by the *cis*-regulatory action of repressors emanating from the various abutting domains. In the following we exclude the first of these alternatives and demonstrate the second (additional evidence pertaining to *onecut* per se will be presented in a forthcoming *cis*-regulatory study). With respect to the control of gene expression within the CB, again several possibilities present themselves. The transcription factor *onecut* could provide the spatial information required for the expression of additional CB genes. Alternatively, these genes might be regulated independently of *onecut*, or a combination of both possibilities might occur, depending on the gene in question. As it turns out, the last is correct, although the second scenario is the more prominent control strategy.

Almost all regulatory genes (here, genes encoding sequence-specific transcription factors) expressed in the embryo up to the stage of gastrulation relevant to this work are known, and are included in our experimental network analyses. To our knowledge, the expression matrix shown in Fig. 3 for the four subdomains of the 35 hpf CB is complete, or nearly so, with respect to the genes expressed within the various territories of the CB, except for subdomain 1. That is, mature GRNs have been published for all the territories of the embryo that border the CB, except for the apical domain through which subdomain 1 passes (Peter et al., 2012; Ben-Tabou de-Leon et al., 2013; Li et al., 2013, 2014). Spatial expression patterns of all the regulatory genes that are transcribed within the CB up to this time are summarized in Fig. 3, which also includes expression data pertaining to genes from immediately neighboring territories (see Fig. 3A,B for simplified embryo maps). The primary RNA *in situ* hybridization data on which the summary is based are shown in supplementary material Fig. S1.

The matrix in Fig. 3C provides the explicit regulatory states of the four regions of the CB up to mid-gastrula, delineated in Fig. 2A,B and Fig. 3B. Remarkably, of the many genes accounted for in this expression matrix, only three are expressed throughout the extent of the CB, as is *onecut*, namely: *z166*, which is expressed in the aboral mesoderm earlier in development (supplementary material Fig. S1J) (Ransick and Davidson, 2012); *otxβ1/2*, which is expressed in the endoderm earlier in development (Yuh et al., 2004; Peter and Davidson, 2011); and *foxg*, which is expressed broadly in the oral ectoderm earlier in development (Li et al., 2014). All of the other regulators transcribed in the CB are expressed only within particular subdomains. The CB is thus, in regulatory terms, a mosaic composed of four separate regulatory states: the oral apical CB (subdomain 1); the bilateral animal lateral CB (subdomain 2); the vegetal lateral CB (subdomain 3); and the vegetal oral CB (subdomain 4). These regulatory states are the sum of the active genes indicated in the respective columns of Fig. 3C. All are complex, indicating different regulatory functions within each subdomain.

Nanostring perturbation analysis

The Nanostring nCounter codeset used for the following measurements contains probes for most *Strongylocentrotus purpuratus* genes that encode transcription factors and signaling ligands expressed up to mid-gastrula stage, except for uncharacterized zinc-finger genes, although all zinc-finger genes encoding proteins orthologous to known transcription factors were included (181 genes in total; for further details see supplementary material Methods and Table S1). The Nanostring instrument, as utilized in this study, provides simultaneous quantitative assessment of the numbers of molecules of each regulatory mRNA species found in control embryos, as compared with embryos of the same batch in which translation of a given regulatory gene has been blocked by introduction of morpholino substituted antisense oligonucleotides (MASOs). Representative results are shown in Fig. 4 (each experiment was multiply replicated, and both splice-blocking and translation-blocking MASOs were evaluated; see Materials and Methods).

Fig. 4A demonstrates that a large fraction of the genes comprising the regulatory states of the CB are responsive to suppression of SoxB1 levels. SoxB1 is a pan-ectodermal transcription factor that is known to affect many other regulatory genes of the oral and aboral ectoderm GRNs (Saudemont et al., 2010; Ben-Tabou de-Leon et al., 2013; Li et al., 2013, 2014). The genes observed to be

Development (2015) 142, 953-961 doi:10.1242/dev.117986

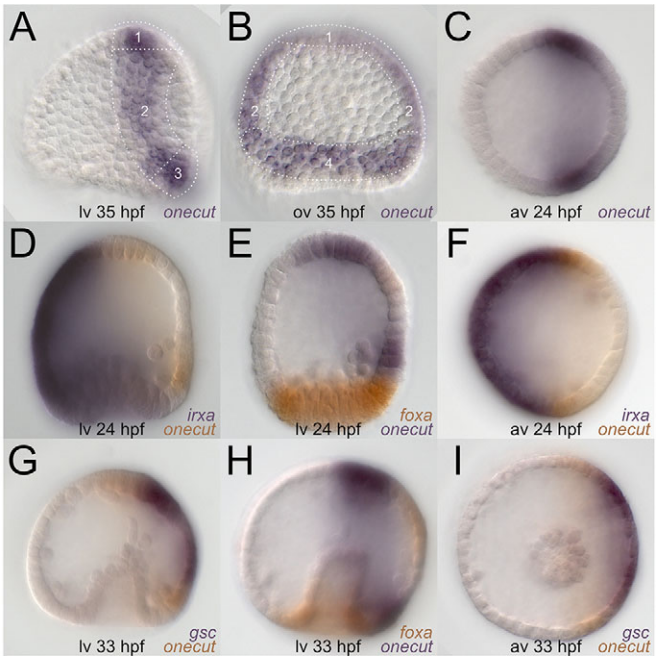

Fig. 2. Delineation of CB subdomains and adjacent embryonic territories. Patterns of gene expression revealed by RNA *in situ* hybridization. (A-C) *onecut* expression pattern in the early gastrula demarcates the cells of the embryo that will give rise to the CB. Four subdomains are identified within the continuous ring of *onecut* transcription. (A) Lateral view of embryo at 35 hpf indicating locations of three of the subdomains: subdomain 1, oral apical; 2, animal lateral; 3, vegetal lateral. (B) Oral view at 35 hpf reveals subdomain 4, vegetal oral. (C) *onecut* expression pattern as viewed from the animal pole at 24 hpf, where the gene is transcribed in the oral portion of the apical plate. (D-I) Patterns of gene expression revealed by double RNA *in situ* hybridization; all images are oriented so that oral ectoderm faces right. (D) Lateral view at 24 hpf. The *irxa* gene (blue) is expressed in aboral ectoderm, and its boundary with subdomain 1 is in focus at the top. Orange, *onecut*. (E) Lateral view at 24 hpf. The *foxa* gene (orange) is expressed in Veg2 endoderm. Two cells separating *foxa* and *onecut* (blue) subdomain 4 on the oral side are Veg1 endoderm, and therefore this region of the CB consists of Veg1 ectoderm (Ransick and Davidson, 1998; Li et al., 2014). (F) View from the animal pole at 24 hpf; in the plane of focus shown, subdomain 2 can be seen to immediately abut the *irxa* (blue) expression domain. Orange, *onecut*. (G) Lateral view at 33 hpf. *gsc* (blue) is expressed in the oral ectoderm; the *gsc* and *onecut* (orange) domains immediately abut at the lower edge of subdomain 1 at the top and at the upper edge of subdomain 4 at the bottom. (H) Lateral view at 33 hpf, early gastrula. Subdomain 4 excludes Veg2 endoderm, but now is clearly in the position of Veg1 ectoderm. Note *foxa* stain (orange) in the future stomodeal region of oral ectoderm. Blue, *onecut*. (I) View from the animal pole at 33 hpf. In the plane of focus shown, the oral *gsc* (blue) expression domain immediately abuts bilateral subdomains 2. Orange, *onecut*.

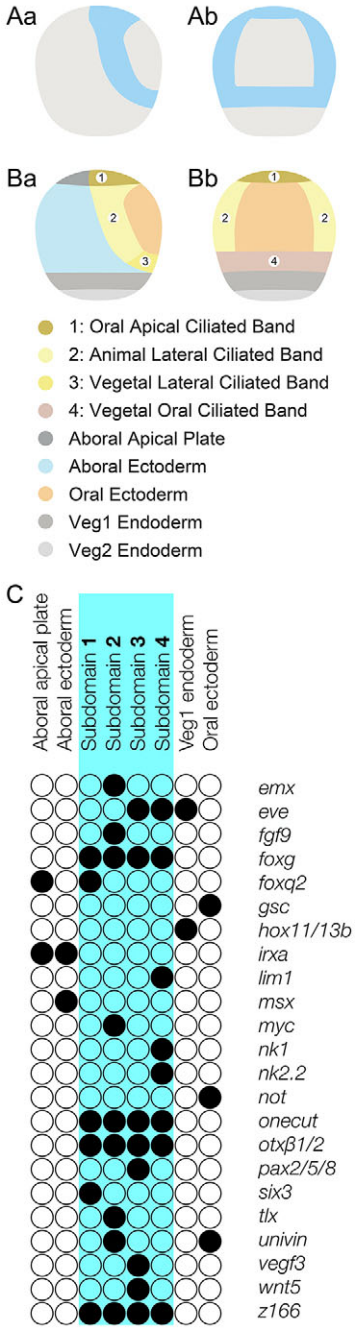

Fig. 3. Schematic representation of CB subdomains and their regulatory states. (A,B) Diagrams of gastrula stage embryo ectodermal regions illustrating the position of the CB subdomains, relative to other select embryonic territories. These diagrams are simplified by omitting territorial subdivisions within the ectoderm (Li et al., 2014). (Aa,b) CB (blue) in lateral and oral views, respectively. (Ba,b) CB subdomains (1-4) and adjacent embryonic territories (color-coded). Lateral and oral views are shown as in A. (C) Regulatory gene expression matrix for CB subdomains and adjacent territories (except for the aboral apical plate, which is not yet completely analyzed) at mid-gastrula. Filled black circles denote gene expression (data from RNA *in situ* hybridizations). Embryonic territories that correspond to the blue CB areas in A are highlighted in blue.

downregulated by *soxb1* MASO are indicated by red dots and in black text (indicating specific relevance to this work) or in gray text (chiefly other ectodermal genes). As these analyses show, SoxB1 controls its own level of expression through negative feedback on the *soxb1* gene, so that *soxb1* MASO produces a large increase in the prevalence of its own mRNA. Furthermore, SoxB1 evidently represses *otxβ1/2* transcription. However, most of its target genes utilize SoxB1 as a transcriptional activator. Two logical consequences follow from these observations. First, since SoxB1 is cleared from the endomesoderm during the blastula stage, which is a prerequisite for endomesodermal development to proceed (Kenny et al., 1999, 2003), its target genes can only be expressed at normal levels in ectodermal, CB, or apical domain cells. This provides a spatial constraint on the expression of SoxB1 target genes adjacent to CB subdomains 3 and 4, both of which abut the Veg1 endoderm. Second, since *soxb1* is expressed everywhere except within the endomesoderm at the time the CB becomes spatially established as a trapezoidal stripe of gene expression (Fig. 1 and Fig. 2A-C), it

Development (2015) 142, 953-961 doi:10.1242/dev.117986

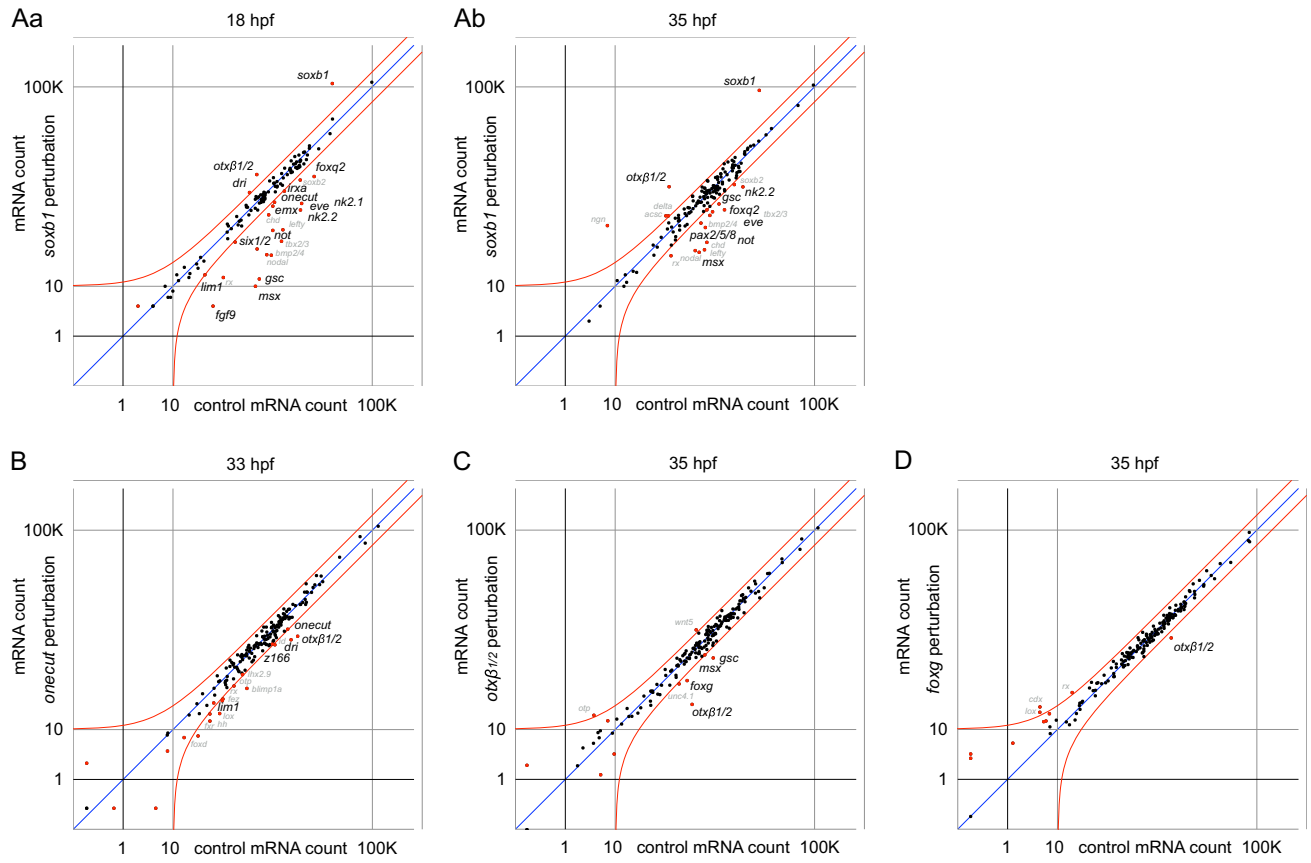

Fig. 4. Nanostring data for effect of MASOs on regulatory mRNA levels. Simultaneous quantitative assessment of transcript levels for 181 regulatory genes and signaling ligands in control embryos and in those bearing MASOs as indicated. Control counts (abscissa) are plotted against experimental counts (ordinate); values shown are counted molecules of each mRNA species per sample. Each sample contained RNA extracted from 33 embryos. Red envelopes indicate the maximum range of scatter as observed in large numbers of control runs with this instrument; from moderate levels of abundance onwards the limit of this variation is approximately twofold. Genes that fall outside these limits are considered to be significantly affected by the MASO treatment. These genes are represented by red dots; those in black text are relevant to the subject of this work, while others are shown in gray. The vast majority of the regulatory genes assessed are expressed the same as in the control in all experiments, and are represented as black dots within the red significance envelope. (Aa,b) Effects of *soxb1* MASO assessed prior to and after CB formation at 18 and 35 hpf, respectively. (B-D) Effects of *onecut* (B), *otxβ1/2* (C) and *foxg* (D) MASOs.

cannot provide spatial boundary information for subdomains 1 and 2, nor for the oral and aboral boundaries of subdomain 3, nor for the oral boundary of subdomain 4. All of these boundaries must therefore be established either by regionally expressed repressors or through positive control via an activator that is in turn confined by gastrula stage to the CB, such as *onecut*. To distinguish between these alternatives, we examined the consequence of blocking *onecut* expression on CB subdomain gene expression, again utilizing Nanostring assays. The other three genes expressed throughout the CB, i.e. *z166*, *otxβ1/2* and *foxg*, are either not uniquely expressed there (as noted above) or their expression within the CB is subsequent to the expression of *onecut*. Therefore, these genes are unlikely candidates to execute early CB-specific spatial control functions. Interference with *z166* expression has no effect on the abundance of any regulatory gene transcript represented in the Nanostring codeset (not shown), and we did not consider its role further.

Despite its precocious activation in the CB, a notable result is that the *onecut* gene does not affect the expression of any of the regulatory genes specifically expressed in any of the CB subdomains (Fig. 4B), except for *onecut* itself, *z166* and *otxβ1/2*. This conclusion was cross-corroborated with two different types of MASO targeted against *onecut* mRNA (translation blocker and splice blocking). Expression of the *deadringer* (*dri*) gene is also downregulated by *onecut* MASO, as previously observed (Saudemont et al., 2010), but expression of *dri* is not exclusively confined to the CB by 35 hpf, as it is then transcribed throughout the oral ectoderm in addition to the CB. Only later in development does *dri* mRNA clear entirely from the oral ectoderm and become CB specific. The other effects of the *onecut* MASO are marginal, or they concern genes expressed in other embryonic territories (shown in gray in Fig. 4B). The *onecut* transcript is present maternally (supplementary material Fig. S2A) and is expressed prior to its zygotic expression in the CB (Otim et al., 2004; Oliveri et al., 2008). Since injected *onecut* MASO is present throughout development, early effects will be recovered here as well as CB-specific effects. Taken together, these results rule out the alternative scenario whereby the spatial pattern of CB gene expression in the four subdomains, each with its own boundaries, is regulated by Onecut. It is clear that this transcription factor does not execute the function of a pioneer gene responsible for delineating the spatial pattern of all subsequent CB gene expression.

Development (2015) 142, 953-961 doi:10.1242/dev.117986

A function that it does perform, however, is indicated in Fig. 4C,D. Here we see that if expression of the Onecut target gene *otxβ1/2* is blocked, the level of *foxg* transcript is significantly decreased. Previous studies have shown that *otxβ1/2* positively autoregulates (Yuh et al., 2004), and this can be seen as well in Fig. 4C. In turn, if expression of *foxg* is blocked (Fig. 4D) the only relevant effect is downregulation of *otxβ1/2*. Thus, *onecut* activates *otxβ1/2*, which in turn activates *foxg*, and *foxg* feeds back on *otxβ1/2*. This feedback loop will be self-perpetuating and, as seen in many other contexts, it can be predicted that it will act to stabilize the CB regulatory state, assuming that the genes of this feedback loop act upon other CB targets later in development. The effect of *onecut* on *foxg* is thus most likely indirect.

Spatial repressors of CB genes

Prior work (Duboc et al., 2010; Li et al., 2013, 2014) has identified several repressors of genes expressed in the CB, and these are specifically listed in the following section. Additional repressive relationships required for given boundaries of CB gene expression are shown in Fig. 5. The initial tier of images in Fig. 5 reveals the response of a *onecut cis*-regulatory construct to the oral repressor Gsc, substantiating at the DNA level an original report that *onecut* expression is excluded from the oral ectoderm by this repressor (Saudemont et al., 2010). In controls the mosaic expression of the *onecut*:GFP *cis*-regulatory module reporter in CB cells is shown in green, superimposed on an RNA *in situ* hybridization image of endogenous *onecut* transcript in red (Fig. 5Aa,a′). But if a cluster of Gsc target sites in this construct is mutated, GFP expression spreads to cells all over the oral face of the embryo (Fig. 5Ab,b′). Thus, we confirm that Gsc directly excludes *onecut* expression from the oral ectoderm, presumably as early as 24 hpf.

Fig. 5B shows representative results with different repressors that affect the boundaries of expression of subdomain 2 genes. In Fig. 5Ba we see that *fgf9* expression is excluded from CB subdomain 1 by Foxq2; in Fig. 5Bb that *fgf9* expression is excluded from the oral face by Not; and in Fig. 5Bc that *fgf9* expression is excluded from subdomains 3 and 4 (Veg1 ectoderm) by Eve. In Fig. 5Bd we see that *myc* expression is excluded from the oral face by Not; and in Fig. 5Be that *myc* expression is also excluded from subdomain 4 by Eve. Similarly, *tlx* expression is excluded from the oral ectoderm by Not (Fig. 5Bf), from the aboral ectoderm by Msx (Fig. 5Bg), and from subdomains 3 and 4 by Eve (Fig. 5Bh). *univin* expression is also excluded from the aboral ectoderm by Msx (Fig. 5Bi). The results shown in Fig. 5 are all those in which spatial exclusion was observed, and negative results in which knockdown of regulatory gene expression had no effect on CB gene transcription domains are not shown. Repressions affecting expression of the key subdomain gene *pax2/5/8* are illustrated in Fig. 5C. Here we see that expression of this gene is excluded from subdomain 4 and the oral face by Not; from the region vegetal to subdomain 3 (i.e. the Veg1 endoderm) by Hox11/13b; and from the aboral ectoderm by an unknown repressor downstream of Bmp2/4 signaling (Fig. 5Ca, Cb and Cc, respectively). Analysis of gene expression patterns (supplementary material Fig. S1) and kinetics (supplementary material Fig. S2) suggests that all of these spatial repressors operate as described above, from 24 hpf until 36 hpf.

Programming CB geometry

A comprehensive list of interactions affecting CB genes of each of the four subdomains is assembled in Table 1. This includes the new observations reproduced in Figs 4 and 5, as well as evidence for specific interactions published previously (Saudemont et al., 2010; Li et al., 2013, 2014). We summarize all of these results in Fig. 6. Here, the four regulatory state subdomains of the CB are represented individually. Impinging on the boundaries are the repressors for which there is evidence that, in their absence, that specific boundary is abrogated, so that expression of the indicated CB gene spreads into the normal domain of expression of the repressor. Obviously, the roster of repressors is not complete, as we lack the identities of the negative inputs that prevent ectopic expression of several of the genes. For instance, in subdomain 2, although we know that Msx represses *tlx* and *univin* expression on the aboral side, as does Irxa repress *onecut*, Msx does not repress *emx*, *fgf9* or *myc* expression on the aboral side and whether this function is executed by Irxa remains unknown. A general feature revealed in this diagram is that the inside boundaries of all four domains, where they abut the oral ectoderm, are defined by only two oral ectoderm repressors, whereas the outer boundaries are controlled by diverse repressors (some of which remain to be identified). Note that in Fig. 6 there is one boundary that is not set negatively, and that is the vegetal boundary of *onecut* expression in subdomains 3 and 4. Here, the probable regulatory limitation precluding more vegetal expression is the absence of SoxB1, which, as discussed above, is cleared in the process of endomesoderm specification.

DISCUSSION

The CB spatial control system in the context of ectoderm GRNs

When the inputs of Fig. 5 and the CB subdomain regulatory states of Fig. 3 are integrated with the published ectoderm GRNs (Ben-Tabou de-Leon et al., 2013; Li et al., 2013, 2014), as well as with not yet published but publically available gene interaction data (http://sugp.caltech.edu/endomes/#EctodermNetwork), a general clarification emerges. It becomes clear why in earlier studies CB boundaries and position within the embryo were found to be affected by perturbation of signaling (for references see Introduction). The reason is that the genes encoding the repressors that establish all of these regulatory state boundaries are direct and indirect transcriptional targets of Nodal and Bmp2/4 signals, in known GRN circuits. Thus, the genomic code that specifies the location of the CB and its boundaries resides physically in the *cis*-regulatory modules of the CB regulatory genes shown within the boxes of Fig. 6. Only one of these genes, *onecut*, has been the subject of direct *cis*-regulatory mutational experimentation to prove the point (Fig. 5A and our unpublished results), but from the other known circuits in which these same repressors operate it is unlikely, for the following reasons, that any of the repressive interactions pictured in Fig. 6 are indirect linkages.

First, it is known that all of these factors also act elsewhere as repressors: in addition to the above references, additional data are available for Not (Materna et al., 2013), Irxa (Saudemont et al., 2010) and Gsc (Angerer et al., 2001; Saudemont et al., 2010). Second, since they act as repressors, in order to function indirectly while retaining the end result of repressing the CB target genes this would require three tandem repressors in sequence, a feature that we have never seen in our GRNs, and neither the expression kinetics of these repressors (supplementary material Fig. S2) nor the wiring of the GRNs as thus far established is consistent with this possibility.

A further clarification is summarized diagrammatically in the GRN map of Fig. 7. Here we see that all of the repressors that generate the boundaries for CB subdomains 1, 2, 3 and 4 emanate from the GRN elements across those respective boundaries. In Fig. 7 the oral and aboral ectoderm GRNs themselves are not shown in

Development (2015) 142, 953-961 doi:10.1242/dev.117986

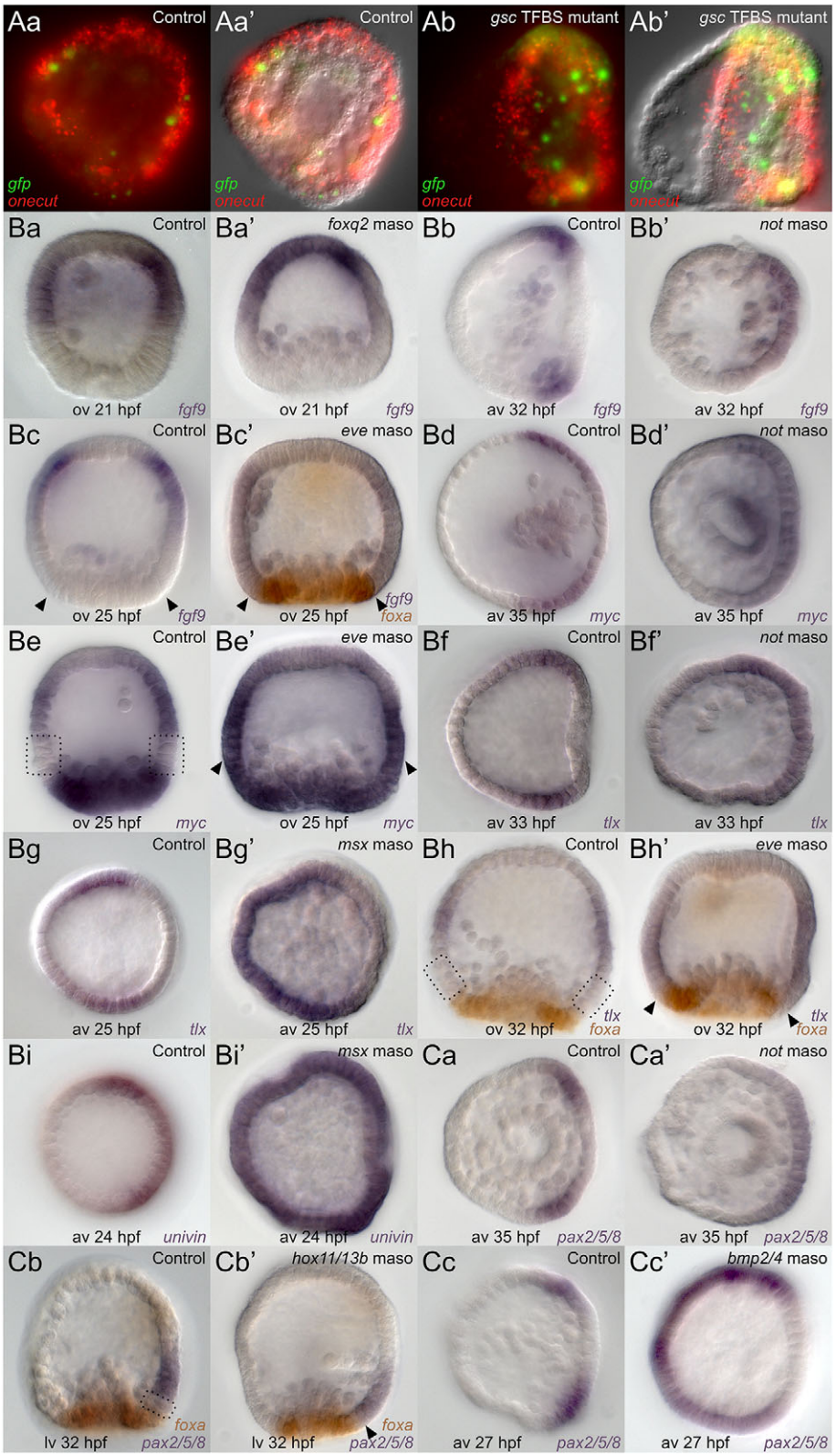

Fig. 5. Repressor-defined CB gene expression boundaries. (A) GFP expression from the *onecut* reporter construct in response to Gsc transcription factor binding site (TFBS) mutation. Endogenous *onecut* expression delineates the CB of a 35 hpf embryo, as shown by fluorescent RNA *in situ* hybridization (red), while a subset of CB cells shown in yellow-green express GFP from the *onecut* reporter construct. (Aa,a′) Fluorescent signal only and fluorescent signal superimposed onto a DIC image, respectively. For the control *onecut* reporter construct note that no green cells are to be seen in the oral face within the CB. (Ab,b′) Fluorescent signal only and fluorescent signal superimposed onto a DIC image, respectively. Same reporter construct as in Aa but with Gsc target sites mutated: cells expressing GFP are now seen throughout the oral face. (B,C) RNA *in situ* hybridization with the indicated probes; orientation: av, animal pole view; lv, lateral view; ov, oral view. (B) Repressors confining expression of subdomain 2 CB genes. (Ba) *fgf9* control and (Ba′) *foxq2* MASO causing *fgf9* expression to spread into subdomain 1. (Bb) *fgf9* control and (Bb′) *not* MASO causing *fgf9* expression to spread across the oral ectoderm. (Bc) *fgf9* control and (Bc′) *eve* MASO causing *fgf9* expression to spread vegetally (arrowheads) so as to include Veg1 ectoderm (of subdomain 3), here seen via double RNA *in situ* hybridization with *foxa* to mark endoderm. (Bd) *myc* control and (Bd′) *not* MASO causing *myc* expression to spread across the oral ectoderm. (Be) *myc* control and (Be′) *eve* MASO causing *myc* expression to spread vegetally (arrowheads) so as to include Veg1 ectoderm (dotted boxes in control). (Bf) *tlx* control and (Bf′) *not* MASO causing *tlx* expression to spread across the oral face. (Bg) *tlx* control and (Bg′) *msx* MASO causing *tlx* expression to spread across the aboral ectoderm. (Bh) *tlx* control and (Bh′) *eve* MASO causing *tlx* expression to spread vegetally (arrowheads) so as to include Veg1 ectoderm (dotted boxes in control), here seen via double RNA *in situ* hybridization with *foxa* to mark endoderm. (Bi) *univin* control and (Bi′) *msx* MASO causing *univin* expression to spread across the aboral ectoderm. (C) Repressors of subdomain 3 genes. (Ca) *pax2*/*5*/*8* control and (Ca′) *not* MASO causing *pax2*/*5*/*8* expression to spread across subdomain 4. (Cb) *pax2*/*5*/*8* control and (Cb′) *hox11*/*13b* MASO causing expression to spread vegetally (arrowhead) to abut endoderm, i.e. to include Veg1 endoderm (dotted box in control), here seen via double RNA *in situ* hybridization with *foxa* to mark endoderm. (Cc) *pax2*/*5*/*8* control and (Cc′) *bmp2*/*4* MASO showing that an unknown aboral ectoderm repressor excludes *pax2*/*5*/*8* from aboral ectoderm.

detail, as they are all to be found elsewhere, and Fig. 7 merely includes the linkages just upstream of the respective repressors. Only the interactions within each of the four CB subdomains are explicitly complete. Note that all subdomains display the *otxβ1/2-foxg* feedback 'motor'; downstream of Onecut expression. The main point illustrated in Fig. 7, however, is that the CB boundaries are, in each subdomain, the specific output of the GRNs creating the regional regulatory states and not the output of the CB subdomains themselves. The circuitry in Fig. 7 shows explicitly the code that results in the observed CB regulatory state geometry. Furthermore, as observed throughout ectodermal GRNs (Li et al., 2014), the general design principle is boundary formation by spatial repressors,

Development (2015) 142, 953-961 doi:10.1242/dev.117986

Table 1. Catalog of regulatory interactions within the CB

#	Interaction	Evidence
Entire CB		
1	*soxb1* activates *onecut*	Fig. 4A; Saudemont et al., 2010
2	*soxb1* activates *emx*	Fig. 4A
3	*soxb1* activates *univin*	Fig. 4A; Saudemont et al., 2010
4	*soxb1* activates *lim1*	Fig. 4A
5	*onecut* activates *z166*	Fig. 4B
6	*onecut* activates *dri*	Fig. 4B; Saudemont et al., 2010
7	*onecut* activates *otxβ1/2*	Fig. 4B
8	*otxβ1/2* activates *otxβ1/2*	Fig. 4C
9	*otxβ1/2* activates *foxg*	Fig. 4C
10	*foxg* activates *otxβ1/2*	Fig. 4D
11	*gsc* represses *onecut*	Fig. 5A; Saudemont et al., 2010
12	*irxa* represses *onecut*	Saudemont et al., 2010
CB1		
13	*emx* represses *foxq2*	Li et al., 2014
14	*not* represses *foxq2*	Li et al., 2014
CB2		
15	*foxq2* represses *emx*	Li et al., 2014
16	*foxq2* represses *fgf9*	Fig. 5Ba
17	*foxq2* represses *univin*	Li et al., 2014
18	*gsc* represses *univin*	Saudemont et al., 2010
19	*not* represses *emx*	Li et al., 2012
20	*not* represses *fgf9*	Fig. 5Bb
21	*not* represses *myc*	Fig. 5Bd
22	*not* represses *tlx*	Fig. 5Bf
23	*msx* represses *tlx*	Fig. 5Bg
24	*msx* represses *univin*	Fig. 5Bi
25	*eve* represses *emx*	Li et al., 2014
26	*eve* represses *fgf9*	Fig. 5Bc
27	*eve* represses *myc*	Fig. 5Be
28	*eve* represses *tlx*	Fig. 5Bh
29	*eve* represses *univin*	Li et al., 2014
CB3		
30	*not* represses *pax2/5/8*	Fig. 5Ca
31	*not* represses *vegf3*	Li et al., 2012
32	*not* represses *wnt5*	Li et al., 2012
33	*hox11/13b* represses *pax2/5/8*	Fig. 5Cb
34	*hox11/13b* represses *vegf3*	Li et al., 2014
CB4		
35	*hox11/13b* represses *lim1*	Li et al., 2014

Thirty-five regulatory interactions, which collectively constitute the CB GRN, are itemized according to the embryonic territory in which they are operative (CB 1, 2, 3, 4 reflect the oral apical, animal lateral, vegetal lateral and vegetal oral CB subdomains, respectively) and the effect that they have on their target gene: interactions 1-10 constitute transcriptional activation, whereas interactions 11-35 constitute transcriptional repression. The data from which each particular interaction was inferred are noted alongside.

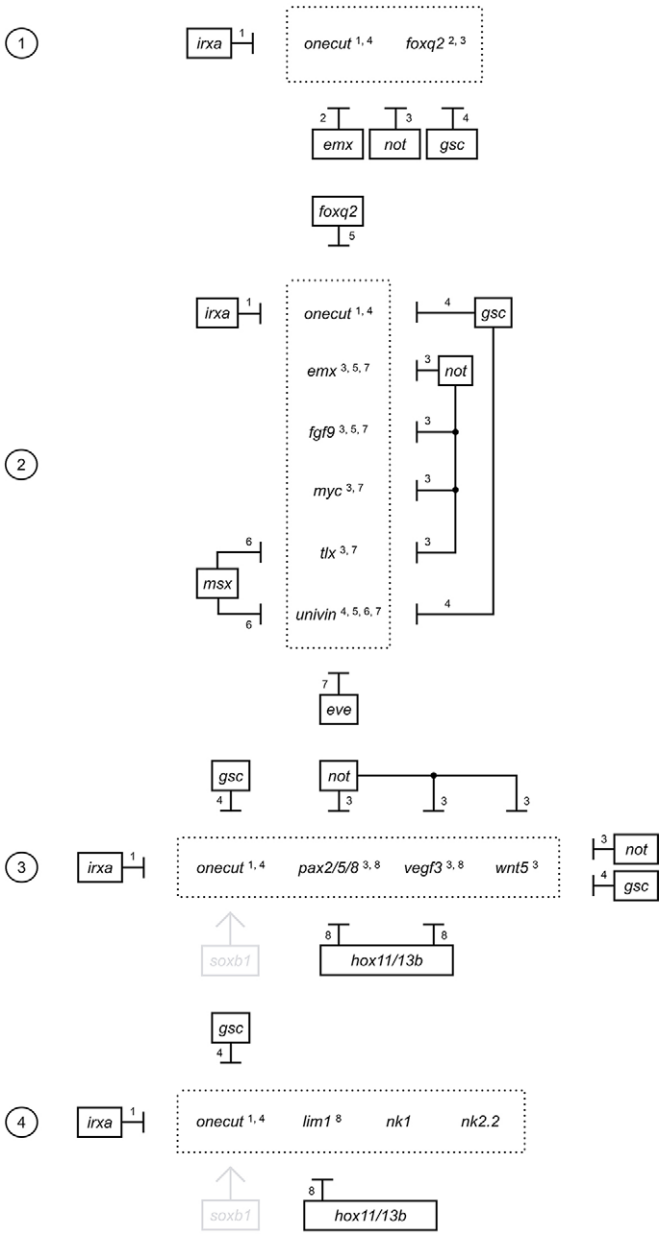

Fig. 6. Summary of repressive interactions that control boundaries of expression of CB genes. The four subdomains of the CB are represented by dotted rectangles: (1) oral apical; (2) animal lateral; (3) vegetal lateral; (4) vegetal oral. Genes of the subdomain regulatory states, from Fig. 3, are shown within. Each domain is oriented with animal boundary facing upwards, oral right (with the exception of subdomains 1 and 4, where oral coincides with vegetal and apical, respectively), aboral left and vegetal down. Repressors expressed across these respective boundaries are listed in black boxes, so as to indicate the orientation of the boundary controls they respectively execute. Data are from Table 1. Numbers relate the given repressors to the genes that they target. Note the mutual repression between *foxq2* and *emx*, which serves to sharpen the boundary between subdomains 1 and 2.

which sharply confine the expression of regulatory genes driven by broadly distributed activators.

Space and complexity

A general import of developmental GRNs is that spatial gene expression always demands a remarkable multiplicity of genomic regulatory transactions. This applies to the complex design of individual *cis*-regulatory modules that execute spatial gene expression, as in the recent illuminating example of the *sparkling* enhancer (Swanson et al., 2010). Even more generally, the same statement applies to the complex information-processing functions of network subcircuits that control spatial gene expression functions by setting boundaries and by installing exclusive spatial regulatory states (Peter and Davidson, 2015). Development of the CB displays both *cis*-regulatory and subcircuit levels of information processing – initially *cis*-regulatory, in the control of the trapezoid stripe of *onecut* gene expression (and the same could potentially be implied for the similar pattern of *z166* expression). We describe how the processing of multiple inputs produces this pattern in a forthcoming *cis*-regulatory study of the *onecut* gene. Here, we focus on the network interaction level of control as it affects four cohorts of gene expression, each of which is confined to the single CB stripe by different combinations of repressive regulators. The spatial coincidence between the expression of the different regulatory genes of each CB

Development (2015) 142, 953-961 doi:10.1242/dev.117986

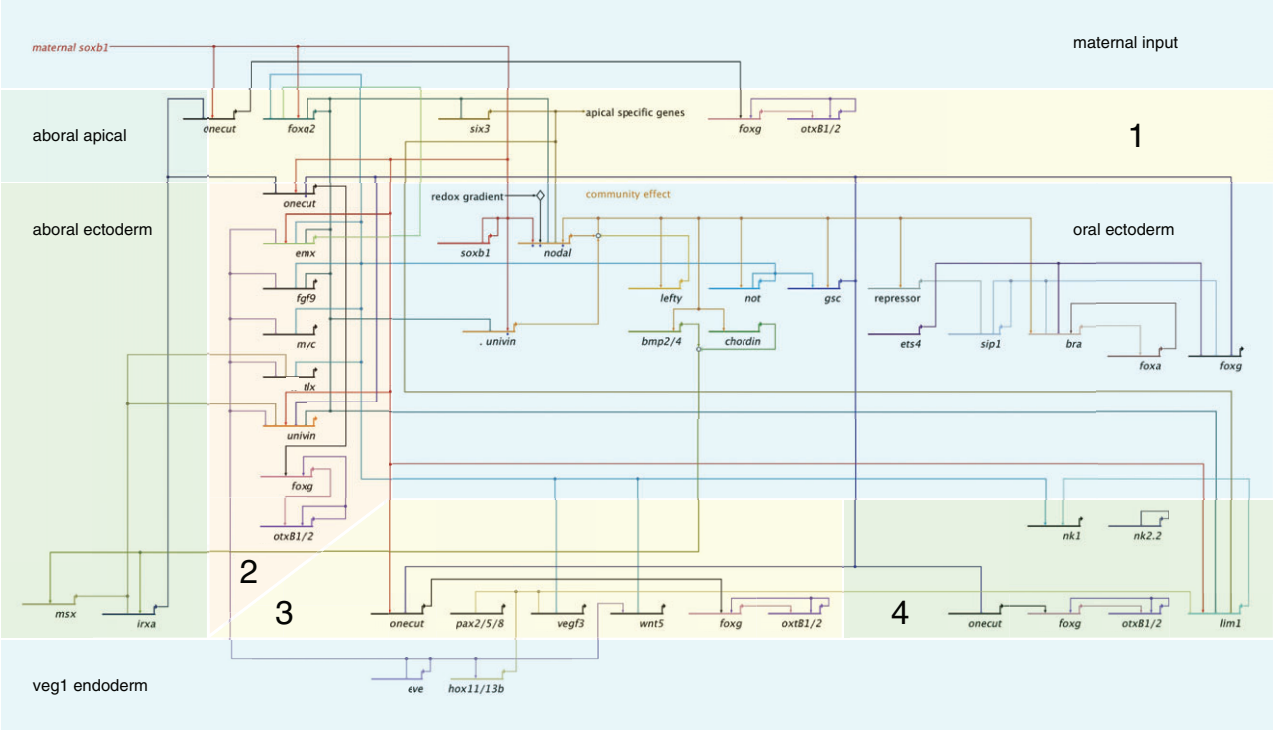

Fig. 7. Spatial control of CB genes by repressors emanating from the oral and aboral ectoderm GRNs, the endomesoderm GRN and the apical domain. Network wiring within the CB is represented in four labeled rectangles, as in Fig. 6, such that (1) denotes oral apical, (2) animal lateral, (3) vegetal lateral and (4) vegetal oral CB. Adjacent embryonic territories are compartmentalized and labeled. External elements of the GRNs abutting the CB shown in this diagram are from previous studies referred to in the text; for current inclusive GRN architecture in interactive format and underlying data see http://sugp.caltech.edu/endomes/. The model is in BioTapestry format (Longabaugh, 2012). It is designed to indicate the genomically encoded sources and targets of the regulatory genes that set the boundaries of the CB regulators, as well as the interactions of the latter among themselves. Compartment colors serve only to differentiate adjacent domains.

subdomain is due to their response to a common set of repressors, some of which are also used by *onecut*. This is also the explanation for the coincidence between the CB stripe and the expression of all the later subdomain genes. One such example is provided by the Gsc repressor, which this and earlier work (Saudemont et al., 2010) showed prevents *onecut* expression in the oral ectoderm, but as we see here the same repressor controls other genes of all four CB subdomains as well.

These encoded, parallel, regulatory relationships ensure the common internal boundaries of the CB regulatory state genes. We can see quantitatively the minimal complexity of this multilevel spatial control system; minimal in that, as Fig. 6 shows, we do not yet know the repressive inputs to several of the CB genes. There are already eight different repressors at play that are required (Fig. 6 and ancillary references), probably directly, to make the CB regulatory state pattern by interacting with the *cis*-regulatory modules of at least a dozen regulatory genes. This example is paradigmatic: when deconvolved into its logical elements (Table 1) the control system consists of as many individual encoded interactions as there are specific regulatory jobs to be done.

MATERIALS AND METHODS

Embryo manipulation

Microinjection of *Strongylocentrotus purpuratus* zygotes was performed according to well-established protocols (McMahon et al., 1985). Eggs were fertilized *in situ* and zygotes injected (1 pl per zygote) with *onecut*: GFP *cis*-regulatory reporter construct or MASOs as follows: *onecut* reporter construct was injected at 1 ng/µl together with 10 ng *Hin*dIII-digested genomic carrier DNA in nuclease-free water; MASOs were injected at 300 µM.

Reporter construct

The wild-type GFP reporter construct contained 311 bp of non-coding sequence, which comprises an enhancer located within the second intron of the *onecut* gene. This DNA sequence element, followed by the GFP coding sequence, was positioned upstream of the *onecut* basal promoter by means of fusion PCR. The mutated version was generated by replacing 52 bp of the enhancer harboring a cluster of consensus Gsc binding sites.

MASOs

The efficacy and specificity of six out of ten MASOs used in this work were authenticated in previous studies, namely those targeting *soxb1*, *bmp2/4*, *eve*, *hox11/13b* (Peter and Davidson, 2011; Li et al., 2014), *foxq2* (Yaguchi et al., 2008) and *not* (Li et al., 2012). Multiple alternative *foxg* MASOs were tested, but only a single translation blocker proved useful: 5′-ACTTCTTGCTAAATACCAAGGCGGA-3′. For *msx*, two translation blockers proved equally useful and produced similar results: 5′-TCGCT-TCAACAGTAATCAAGGATGA-3′ and 5′-TGCACGTCGATTCGATA-GAAGAAAA-3′; data shown in Fig. 5 were obtained using the first of these. For *otxβ1/2*, a single translation blocker proved useful: 5′-AATGGTGTAAGCCATGCTCGCTACC-3′. For knockdown of *onecut* expression, we identified both a splice-blocking (5′-CAAGTTTTTG-ACTGACTTACCAGCT-3′) and a translation-blocking (5′-AGCCAAC-TAACTCACTTGAAAGCAT-3′) MASO, which gave similar results, cross-validating one another.

Nanostring nCounter analysis

Embryos were manually harvested at the desired developmental stage. Samples were prepared containing 100 embryos in 15 µl RLT Plus buffer (Qiagen) with 2-mercaptoethanol (1:100) and stored at −70°C. Once thawed, 5 µl lysate was processed following the nCounter manufacturer's instructions (Nanostring Technologies). Detailed information concerning the Nanostring probe set utilized in this study, normalization of mRNA raw

code counts, and threshold parameters, is given in supplementary material Methods and Table S1. Relevant Nanostring data have been deposited at the Dryad Digital Repository under data identifier doi:10.5061/dryad.mb804.

RNA *in situ* hybridization

Whole-mount RNA *in situ* hybridization was performed following our previously published method (Ransick, 2004). The probes used in this study were complementary to almost the entire coding sequence of all mRNAs targeted, the sequences of which are available at http://www.spbase.org:3838/quantdev (Tu et al., 2014).

Acknowledgements

We thank Eric Erkenbrack for the microphotograph shown in Fig. 1A and Klara Stefflova for assistance throughout figure preparation.

Competing interests

The authors declare no competing or financial interests.

Author contributions

J.C.B. and E.H.D. designed the research; J.C.B. and E.L. performed the research; J.C.B., E.L. and E.H.D. analyzed the data; and J.C.B. and E.H.D. wrote the paper.

Funding

This research was supported by the National Institutes of Health [HD067454 to E.H.D.]. Deposited in PMC for release after 12 months.

Supplementary material

Supplementary material available online at
http://dev.biologists.org/lookup/suppl/doi:10.1242/dev.117986/-/DC1

References

Angerer, L. M., Oleksyn, D. W., Levine, A. M., Li, X., Klein, W. H. and Angerer, R. C. (2001). Sea urchin goosecoid function links fate specification along the animal-vegetal and oral-aboral embryonic axes. *Development* **128**, 4393-4404.

Angerer, L. M., Yaguchi, S., Angerer, R. C. and Burke, R. D. (2011). The evolution of nervous system patterning: insights from sea urchin development. *Development* **138**, 3613-3623.

Ben-Tabou de-Leon, S., Su, Y.-H., Lin, K.-T., Li, E. and Davidson, E. H. (2013). Gene regulatory control in the sea urchin aboral ectoderm: spatial initiation, signaling inputs, and cell fate lockdown. *Dev. Biol.* **374**, 245-254.

Duboc, V., Röttinger, E., Besnardeau, L. and Lepage, T. (2004). Nodal and BMP2/4 signaling organizes the oral-aboral axis of the sea urchin embryo. *Dev. Cell* **6**, 397-410.

Duboc, V., Lapraz, F., Besnardeau, L. and Lepage, T. (2008). Lefty acts as an essential modulator of Nodal activity during sea urchin oral-aboral axis formation. *Dev. Biol.* **320**, 49-59.

Duboc, V., Lapraz, F., Saudemont, A., Bessodes, N., Mekpoh, F., Haillot, E., Quirin, M. and Lepage, T. (2010). Nodal and BMP2/4 pattern the mesoderm and endoderm during development of the sea urchin embryo. *Development* **137**, 223-235.

Howard-Ashby, M., Materna, S. C., Brown, C. T., Chen, L., Cameron, R. A. and Davidson, E. H. (2006). Identification and characterization of homeobox transcription factor genes in Strongylocentrotus purpuratus, and their expression in embryonic development. *Dev. Biol.* **300**, 74-89.

Kenny, A. P., Kozlowski, D., Oleksyn, D. W., Angerer, L. M. and Angerer, R. C. (1999). SpSoxB1, a maternally encoded transcription factor asymmetrically distributed among early sea urchin blastomeres. *Development* **126**, 5473-5483.

Kenny, A. P., Oleksyn, D. W., Newman, L. A., Angerer, R. C. and Angerer, L. M. (2003). Tight regulation of SpSoxB factors is required for patterning and morphogenesis in sea urchin embryos. *Dev. Biol.* **261**, 412-425.

Lapraz, F., Besnardeau, L. and Lepage, T. (2009). Patterning of the dorsal-ventral axis in echinoderms: insights into the evolution of the BMP-chordin signaling network. *PLoS Biol.* **7**, e1000248.

Li, E., Materna, S. C. and Davidson, E. H. (2012). Direct and indirect control of oral ectoderm regulatory gene expression by Nodal signaling in the sea urchin embryo. *Dev. Biol.* **369**, 377-385.

Li, E., Materna, S. C. and Davidson, E. H. (2013). New regulatory circuit controlling spatial and temporal gene expression in the sea urchin embryo oral ectoderm GRN. *Dev. Biol.* **382**, 268-279.

Li, E., Cui, M., Peter, I. S. and Davidson, E. H. (2014). Encoding regulatory state boundaries in the pregastrular oral ectoderm of the sea urchin embryo. *Proc. Natl. Acad. Sci. USA* **111**, E906-E913.

Longabaugh, W. J. (2012). BioTapestry: a tool to visualize the dynamic properties of gene regulatory networks. *Methods Mol. Biol.* **786**, 359-394.

Materna, S. C., Ransick, A., Li, E. and Davidson, E. H. (2013). Diversification of oral and aboral mesodermal regulatory states in pregastrular sea urchin embryos. *Dev. Biol.* **375**, 92-104.

McMahon, A. P., Flytzanis, C. N., Hough-Evans, B. R., Katula, K. S., Britten, R. J. and Davidson, E. H. (1985). Introduction of cloned DNA into sea urchin egg cytoplasm: replication and persistence during embryogenesis. *Dev. Biol.* **108**, 420-430.

Oliveri, P., Tu, Q. and Davidson, E. H. (2008). Global regulatory logic for specification of an embryonic cell lineage. *Proc. Natl. Acad. Sci. USA* **105**, 5955-5962.

Otim, O., Amore, G., Minokawa, T., McClay, D. R. and Davidson, E. H. (2004). SpHnf6, a transcription factor that executes multiple functions in sea urchin embryogenesis. *Dev. Biol.* **273**, 226-243.

Peter, I. S. and Davidson, E. H. (2011). A gene regulatory network controlling the embryonic specification of endoderm. *Nature* **474**, 635-639.

Peter, I. S. and Davidson, E. H. (2015). *Genomic Control Process, Development and Evolution*. Oxford: Academic Press, Elsevier.

Peter, I. S., Faure, E. and Davidson, E. H. (2012). Predictive computation of genomic logic processing functions in embryonic development. *Proc. Natl. Acad. Sci. USA* **109**, 16434-16442.

Poustka, A. J., Kühn, A., Radosavljevic, V., Wellenreuther, R., Lehrach, H. and Panopoulou, G. (2004). On the origin of the chordate central nervous system: expression of onecut in the sea urchin embryo. *Evol. Dev.* **6**, 227-236.

Poustka, A. J., Kühn, A., Groth, D., Weise, V., Yaguchi, S., Burke, R. D., Herwig, R., Lehrach, H. and Panopoulou, G. (2007). A global view of gene expression in lithium and zinc treated sea urchin embryos: new components of gene regulatory networks. *Genome Biol.* **8**, R85.

Ransick, A. (2004). Detection of mRNA by in situ hybridization and RT-PCR. *Methods Cell Biol.* **74**, 601-620.

Ransick, A. and Davidson, E. H. (1998). Late specification of Veg1 lineages to endodermal fate in the sea urchin embryo. *Dev. Biol.* **195**, 38-48.

Ransick, A. and Davidson, E. H. (2012). Cis-regulatory logic driving glial cells missing: self-sustaining circuitry in later embryogenesis. *Dev. Biol.* **364**, 259-267.

Saudemont, A., Haillot, E., Mekpoh, F., Bessodes, N., Quirin, M., Lapraz, F., Duboc, V., Röttinger, E., Range, R., Oisel, A. et al. (2010). Ancestral regulatory circuits governing ectoderm patterning downstream of Nodal and BMP2/4 revealed by gene regulatory network analysis in an echinoderm. *PLoS Genet.* **6**, e1001259.

Su, Y.-H., Li, E., Geiss, G. K., Longabaugh, W. J. R., Krämer, A. and Davidson, E. H. (2009). A perturbation model of the gene regulatory network for oral and aboral ectoderm specification in the sea urchin embryo. *Dev. Biol.* **329**, 410-421.

Swanson, C. I., Evans, N. C. and Barolo, S. (2010). Structural rules and complex regulatory circuitry constrain expression of a Notch- and EGFR-regulated eye enhancer. *Dev. Cell* **18**, 359-370.

Tu, Q., Cameron, R. A. and Davidson, E. H. (2014). Quantitative developmental transcriptomes of the sea urchin Strongylocentrotus purpuratus. *Dev. Biol.* **385**, 160-167.

Yaguchi, S., Yaguchi, J., Angerer, R. C. and Angerer, L. M. (2008). A Wnt-FoxQ2-nodal pathway links primary and secondary axis specification in sea urchin embryos. *Dev. Cell* **14**, 97-107.

Yaguchi, S., Yaguchi, J., Angerer, R. C., Angerer, L. M. and Burke, R. D. (2010). TGFβ signaling positions the ciliary band and patterns neurons in the sea urchin embryo. *Dev. Biol.* **347**, 71-81.

Yuh, C.-H., Dorman, E. R., Howard, M. L. and Davidson, E. H. (2004). An otx cis-regulatory module: a key node in the sea urchin endomesoderm gene regulatory network. *Dev. Biol.* **269**, 536-551.

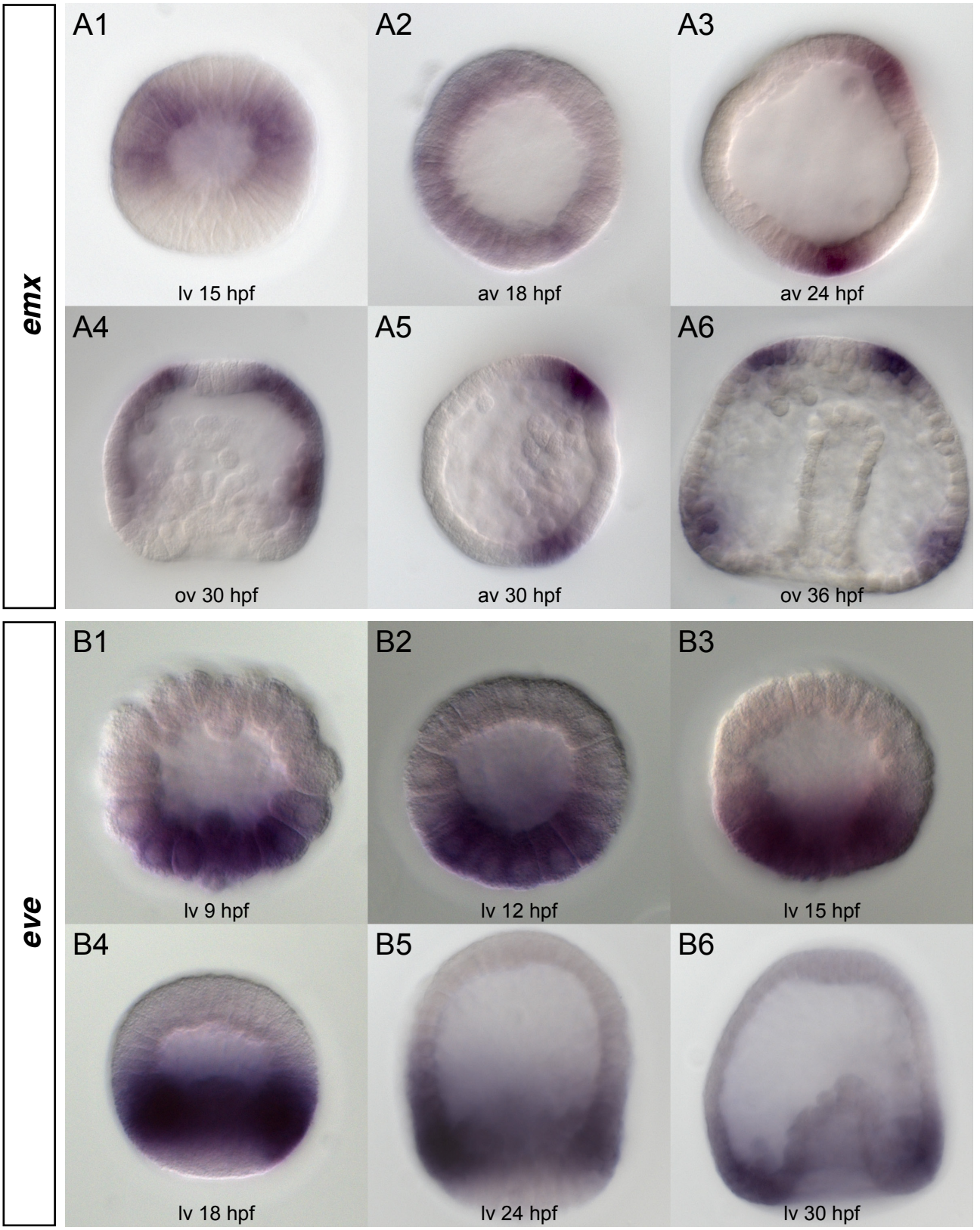
emx
A1
lv 15 hpf
A2
av 18 hpf
A3
av 24 hpf
A4
ov 30 hpf
A5
av 30 hpf
A6
ov 36 hpf
eve
B1
lv 9 hpf
B2
lv 12 hpf
B3
lv 15 hpf
B4
lv 18 hpf
B5
lv 24 hpf
B6
lv 30 hpf

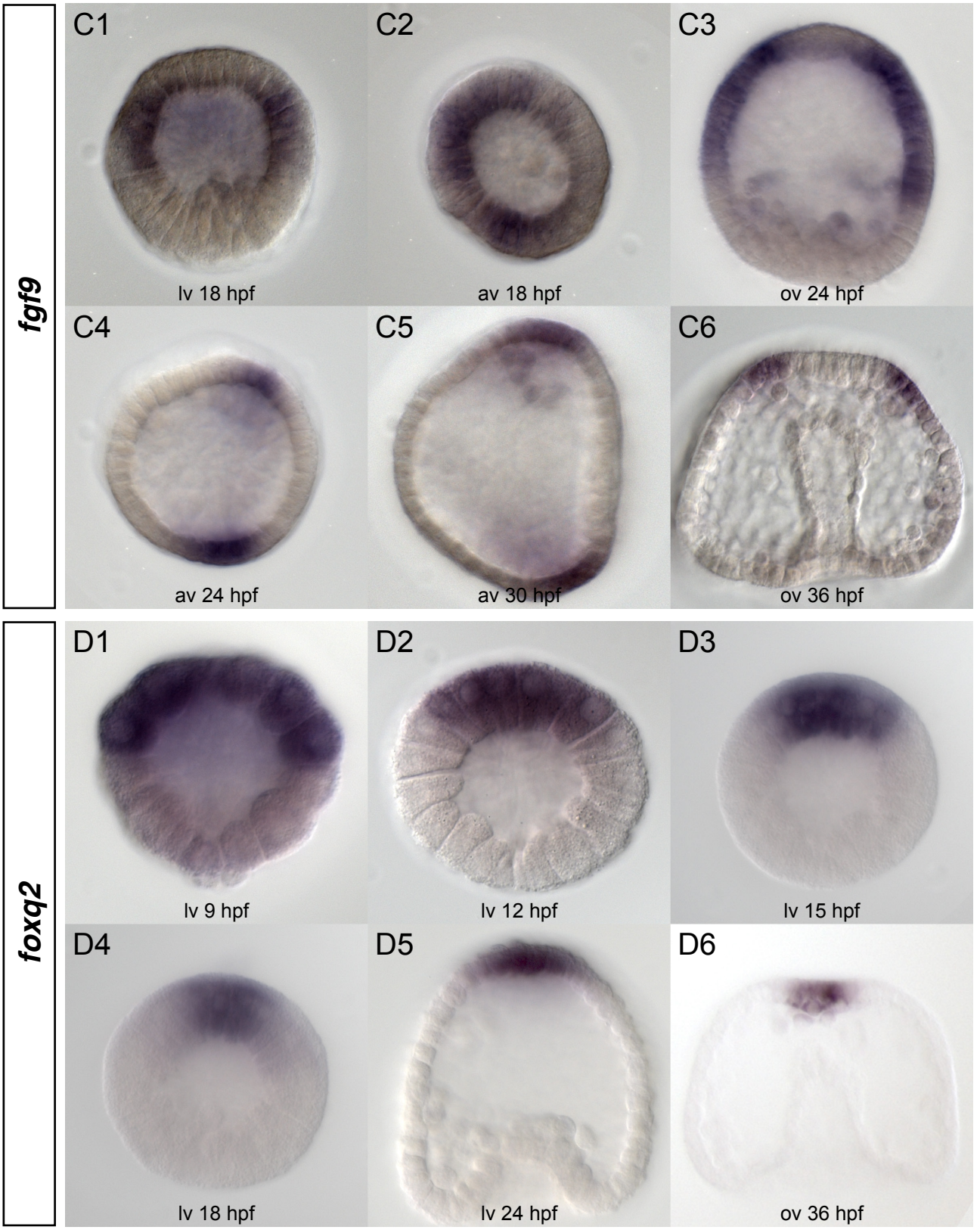
fgf9
C1
lv 18 hpf
C2
av 18 hpf
C3
ov 24 hpf
C4
av 24 hpf
C5
av 30 hpf
C6
ov 36 hpf
foxq2
D1
lv 9 hpf
D2
lv 12 hpf
D3
lv 15 hpf
D4
lv 18 hpf
D5
lv 24 hpf
D6
ov 36 hpf

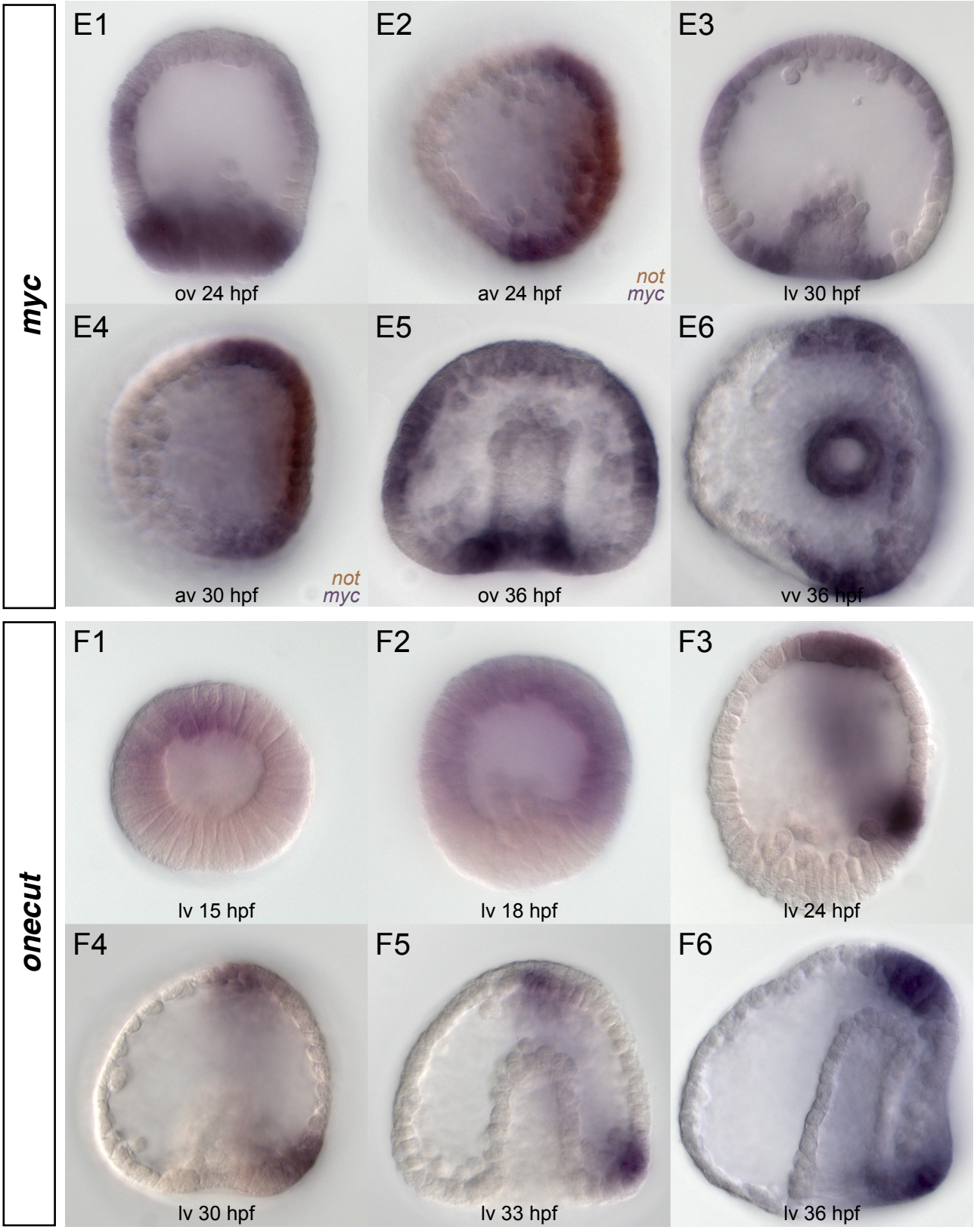
myc
E1
ov 24 hpf
E2
av 24 hpf
not myc
E3
lv 30 hpf
E4
av 30 hpf
not myc
E5
ov 36 hpf
E6
vv 36 hpf
onecut
F1
lv 15 hpf
F2
lv 18 hpf
F3
lv 24 hpf
F4
lv 30 hpf
F5
lv 33 hpf
F6
lv 36 hpf

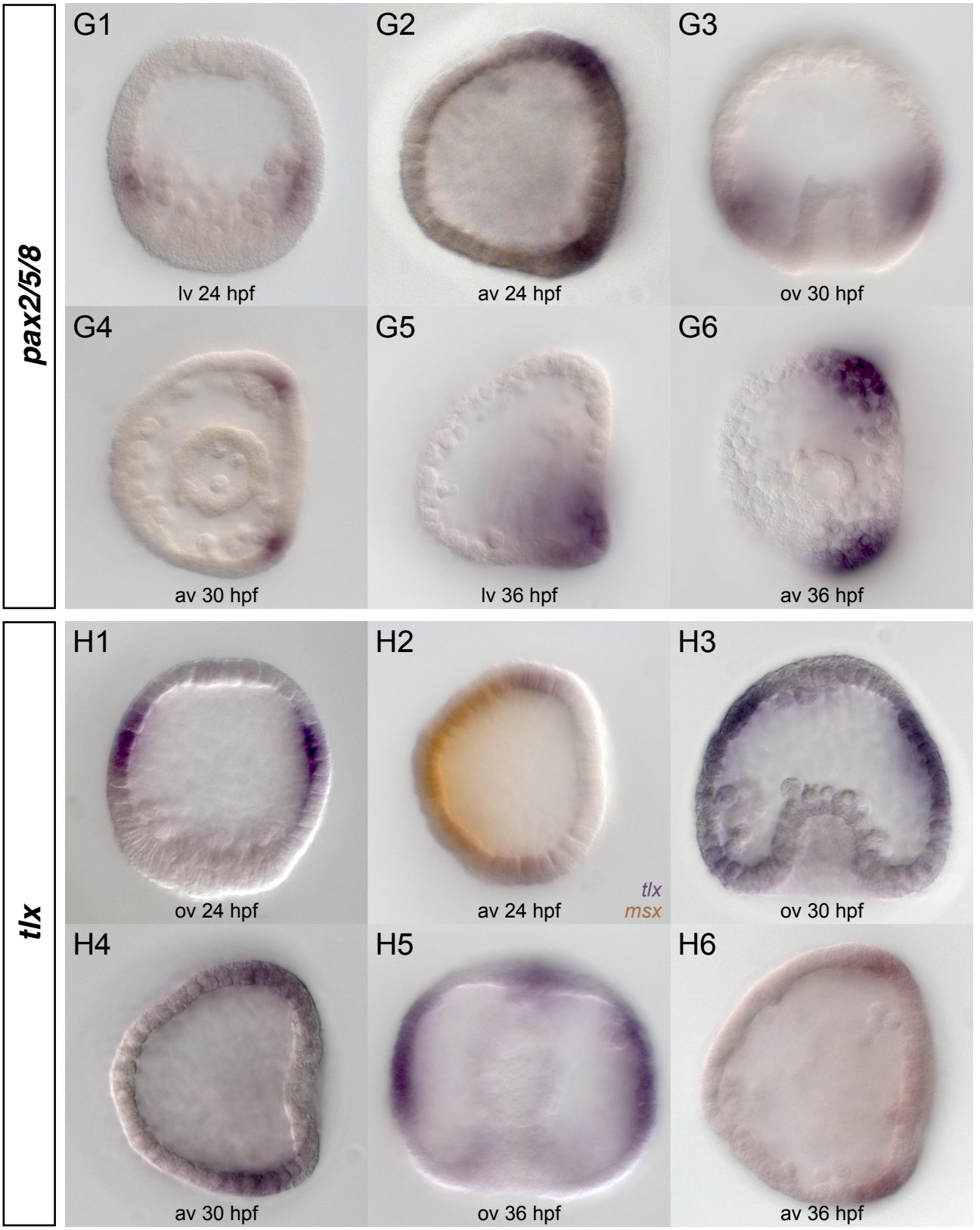
pax2/5/8
G1
lv 24 hpf
G2
av 24 hpf
G3
ov 30 hpf
G4
av 30 hpf
G5
lv 36 hpf
G6
av 36 hpf
tlx
H1
ov 24 hpf
H2
av 24 hpf
tlx
msx
H3
ov 30 hpf
H4
av 30 hpf
H5
ov 36 hpf
H6
av 36 hpf

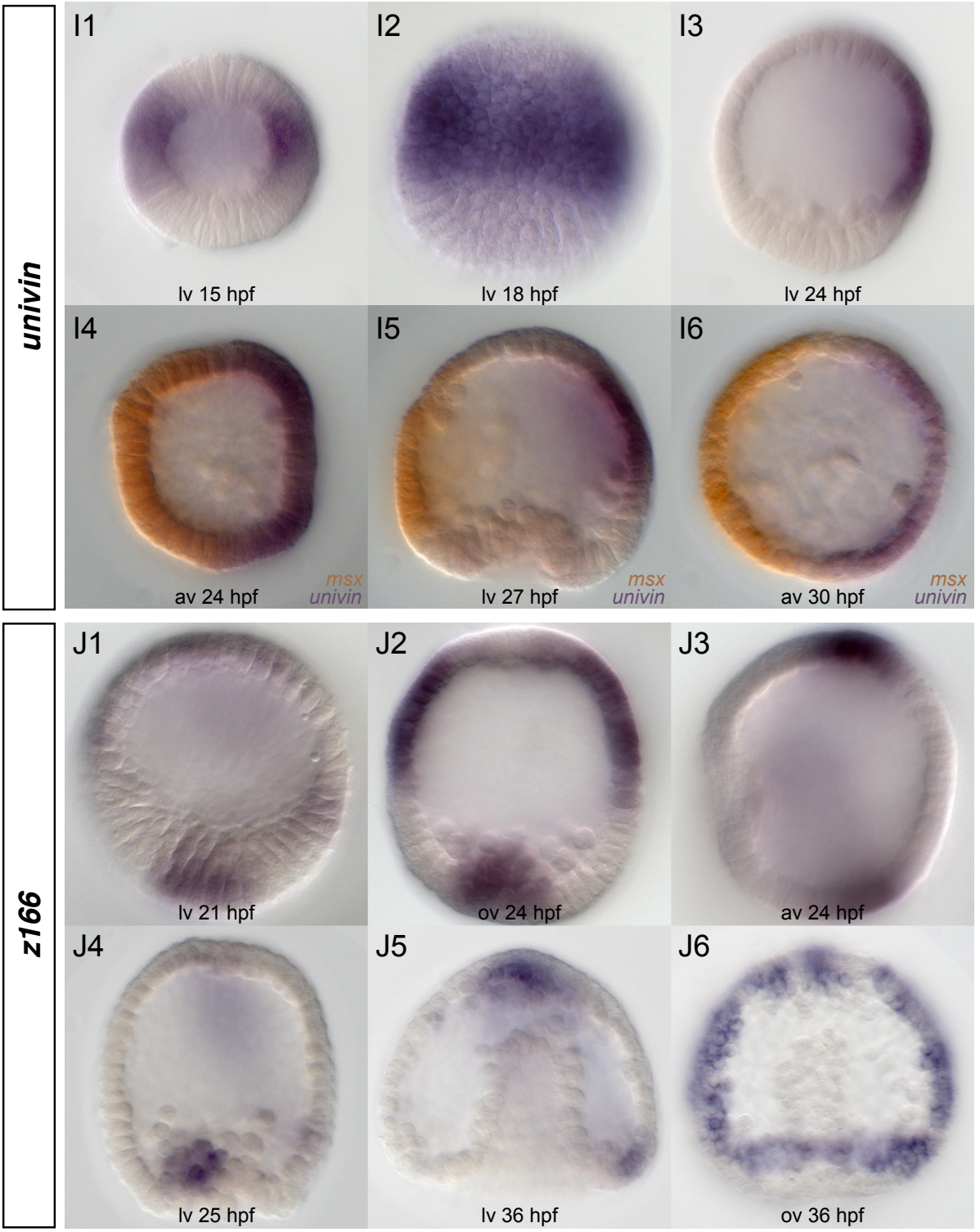

Supplementary Fig. S1. Gene expression patterns. (A-J) RNA *in situ* hybridization series for relevant genes (A) *emx*, (B) *eve*, (C) *fgf9*, (D) *foxq2*, (E) *myc*, (F) *onecut*, (G) *pax2/5/8*, (H) *tlx*, (I) *univin*, (J) *z166*. Abbreviations: av, apical pole view; lv, lateral view; ov, oral view; vv, ventral view; hpf, hours post fertilization. Oral ectoderm faces towards the right, except in panels marked ov, where the oral ectoderm is viewed head-on.

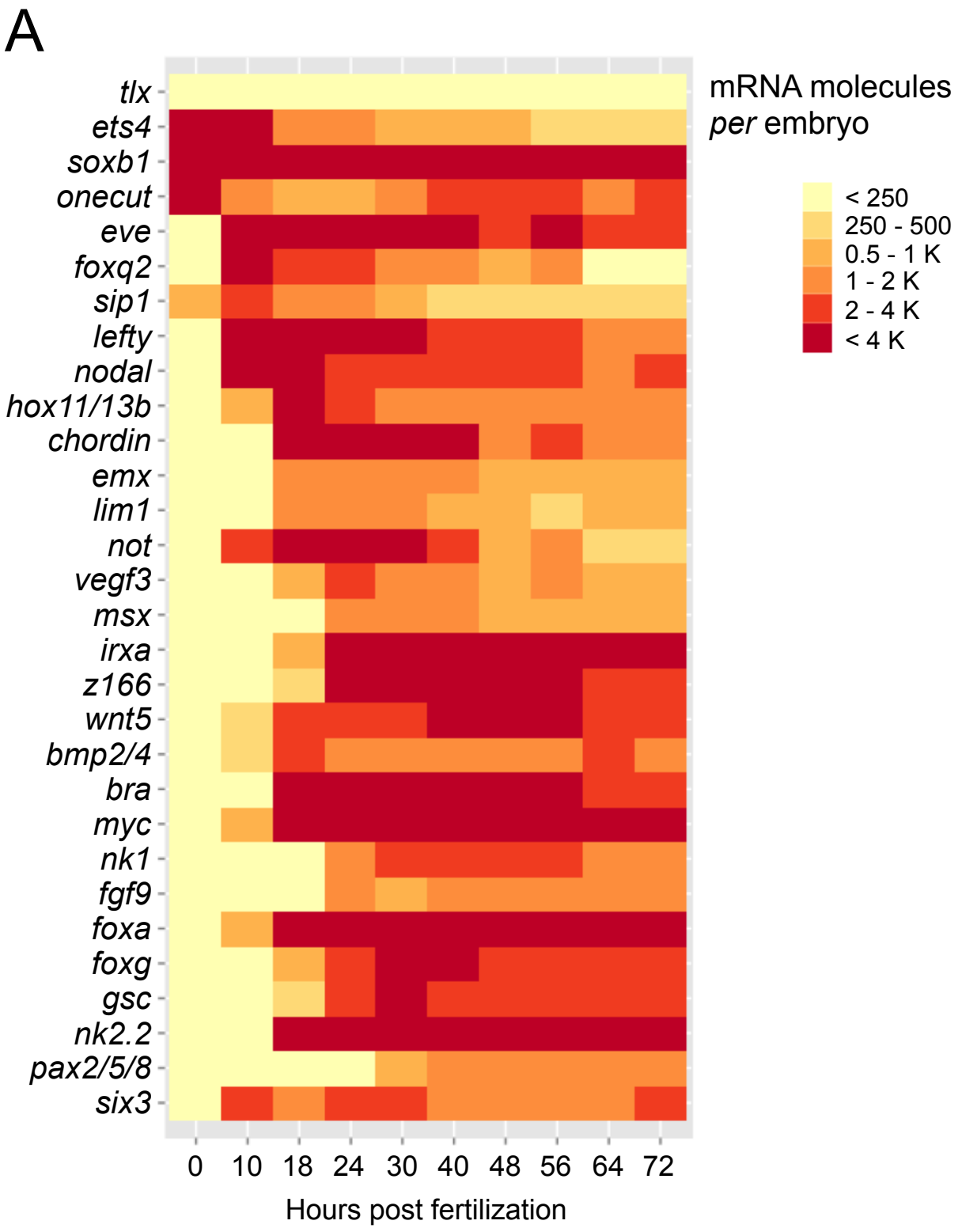
A
tlx
ets4
soxb1
onecut
eve
foxq2
sip1
lefty
nodal
hox11/13b
chordin
emx
lim1
not
vegf3
msx
irxa
z166
wnt5
bmp2/4
bra
myc
nk1
fgf9
foxa
foxg
gsc
nk2.2
pax2/5/8
six3
0
10
18
24
30
40
48
56
64
72
Hours post fertilization
mRNA molecules
per embryo
< 250
250 - 500
0.5 - 1 K
1 - 2 K
2 - 4 K
< 4 K

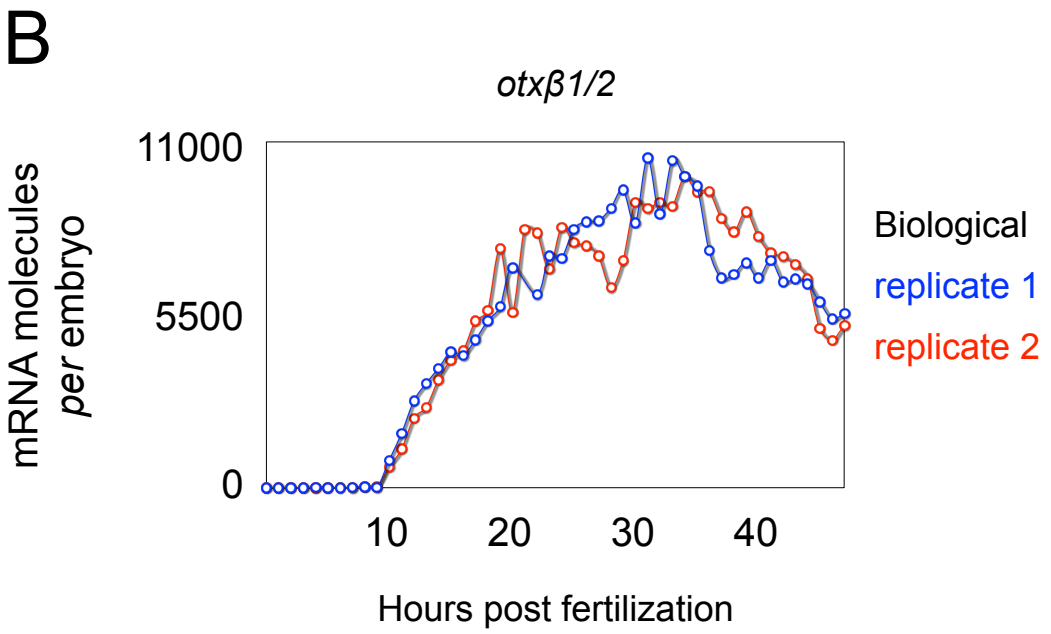

Supplementary Fig. S2. Gene expression kinetics. (A) Level of mRNA abundance throughout development for all genes modeled in Fig. 7. Heat-map reflecting the expression profile for each gene listed. Absolute values of mRNA levels are inferred from the color code key, at right. Measurements are from our previous study (Tu et al., 2014), and are plotted using the online tool described therein. (B) Expression time course for the *otxβ1/2* splice variant (this transcript is not included in A). Data are from previously published measurements (Materna et al., 2010).

Table S1. Nanostring codeset information (mRNA targets 1-197)

Click here to Download Table S1

Supplementary Methods

Normalization

mRNA raw code counts (RCCs) were normalized as described (Barsi et al., 2014).

Differential gene expression

Given the vast experience our laboratory has amassed over the years concerning this technology and the fact that we contributed toward it's pioneer study (Geiss et al., 2008), hundreds of technical replicates have been compared using the nCounter analysis system. In no instance has the code count between technical replicates, for any given mRNA species in our codeset, deviated beyond twofold (with the exception of insignificantly low-level transcripts). From this, we conclude that differential gene expression is biologically relevant if a delta larger than twofold is observed for any given transcript. We acknowledge that our assumption is conservative, given that transcripts with a smaller observed delta could potentially be statistically significant. Nevertheless, for the purpose of this study, there is no question that a twofold difference (or higher) in gene expression accurately reflects the biological repercussion of a MASO perturbation experiment. The envelope delineated by a red line in Fig. 4 reflects the empirically derived confidence threshold described above. Data points found beyond this envelope are of biological import to this study.

References

Barsi, J. C., Tu, Q. and Davidson, E. H. (2014). General approach for in vivo recovery of cell type-specific effector gene sets. *Genome Res*. **24**, 860-868.

Geiss, G. K., Bumgarner, R. E., Birditt, B., Dahl, T., Dowidar, N., Dunaway, D. L., Fell, H. P., Ferree, S., George, R. D., Grogan, T. et al. (2008). Direct multiplexed measurement of gene expression with color-coded probe pairs. *Nat. Biotechnol.* **26**, 317-325.

Materna, S. C., Nam, J. and Davidson, E. H. (2010). High accuracy, high-resolution prevalence measurement for the majority of locally expressed regulatory genes in early sea urchin development. *Gene Expr. Patterns* **10**, 177-184.